Ti-2007 Science and Technology, edited by M. Ninomi, S. Akiyama, M. Ikeda, M. Hagiwara, K. Maruyama
The Japan Institute of Metals (2007)

Investigating Microstructural Evolution in the Near Alpha Alloy Timetal® 834 using Electron Back Scatter Diffraction (EBSD)

Peter Davies[1], Brad Wynne[1], W. Mark Rainforth[1]

[1]IMMPETUS *(Institute for Microstructural and Mechanical Process Engineering: The University of Sheffield), Mappin Street, Sheffield 51 3JD, UK*

Microstructural evolution in Timetal® 834 was investigated using plane strain compression tests for a deformation temperature of 1010°C at an equivalent tensile strain rate of $2s^{-1}$ and equivalent strains up to 1.23. Microstructures were investigated using optical microscopy and EBSD. In addition, a computer program was written to reconstruct the parent β phase from a standard EBSD analysis of the transformed microstructures. At the test temperature of 1010°C, the microstructures consisted of primary alpha (α_P) grains in a continuous β matrix. The α_P grains only contributed a small amount to the overall strain, with the majority of the strain accommodated by the β phase. The majority of the α_P phase remained unrecrystallized. However, deformation in the α_P phase was very heterogeneous and at high strains a form of dynamic recrystallization was observed in small areas of heavy localized deformation. The reconstructed β phase revealed mixed microstructures of dynamically recrystallized grains necklaced around larger deformed grains. The heterogeneous nature of the dynamic recrystallization suggests that the β phase deforms inhomogeneously due to the accommodation strains imposed by the α_P phase.

Keywords: *titanium (Ti), Timetal® 834, electron back scatter diffraction (EBSD), recrystallization, thermomechanical processing.*

1. Introduction

Titanium and its alloys exhibit between 900°C and 1000°C an α→β phase transformation on heating and a β→α transformation on cooling. Standard EBSD analysis allows the characterization of the microtexture of the primary alpha (α_p) phase but can only provide limited information about the high temperature β phase because this transforms on cooling to form an inherited secondary alpha (α_s) phase.

Humbert et al.[1,2] proposed a scheme to obtain the parent β grain orientation from a small number of inherited α_s variants in transformed microstructures. This method is well suited to cases in which the orientation relation between parent and variants is strict or quasi-strict.

Later work[3,4] described automated procedures for reconstructing EBSD maps of the parent β microtexture from a standard EBSD analysis of the inherited α_s microtexture. In this work, the reconstruction method used all of the available α_s orientation data within a parent β grain to calculate an average β orientation for the grain. This approach is better adapted to deal with cases where the Burgers orientation relation is not so strictly observed. However, since each reconstructed β grain has only an average orientation, it does not reveal as much information on orientation distributions that may exist within β grains.

In this study, we adapted the scheme proposed in the earlier work in a way that enabled us to calculate a unique parent β orientation for each α_s pixel in the map. This approach, when used with a fine water quenched α_s microstructure and high resolution EBSD analysis, allows information on the deformation substructure within parent β grains to be revealed.

2. Experimental Procedures

2.1 Starting Material

Timetal® 834 (Ti-5.8%Al-4%Sn-3.5%Zr-0.7%Nb-0.5% Mo-0.35%Si-0.06%C) was received in billet form. The β transus was approximately 1050°C. The microstructure was bimodal consisting of 75% α_p and 25% coarse α_s colonies.

2.2 Thermomechanical Testing

A schematic of the plane strain compression (PSC) test is shown in Fig. la. PSC specimens, measuring 60x30x10 cm were machined from the billet such that the PSC normal direction was parallel to the billet axis (Fig. lb). PSC tests were conducted on a Servotest Thermomechanical Compression Machine fitted with an induction heating unit for fast and accurate control of the specimen temperature. Specimen temperature was monitored by a thermocouple fitted into a small hole near the centre of the deformation zone. To reduce friction, the specimens were coated in a thin layer of AMLUBE 1000 glass lubricant.

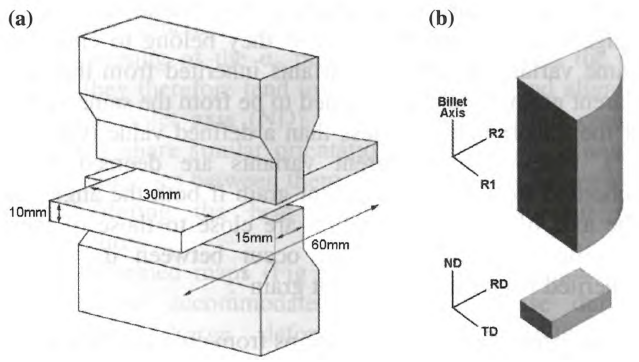

Figure 1. (a) Schematic diagram of the plane strain compression test, (b) Orientation of the PSC specimens with respect to the billet.

Test conditions were for an α+β forging corresponding to the simulation of closed-die forging to a final shape. The tests were conducted at an initial deformation temperature of 1010°C after holding for 10 min at temperature. Tests were performed at a constant equivalent tensile strain rate of 2 s^{-1} to equivalent strains (ε_{vm}) of 0.64 and 1.23 followed by water quenching. A specimen was also water quenched just before deformation to quantify the initial microstructure of the undeformed material.

2.3. Microstructural Characterization

2.3.1. Metallographic Evaluation

Sections in the ND/RD plane were cut from the centre of the specimen width and prepared using techniques outlined by Thomas et al.[5].

2.3.2. Electron Back Scatter Diffraction

EBSD analysis was carried out on an FEI Sirion FEG SEM, equipped with a fully automatic HKL Technology EBSD system, operated at 15kV. Orientation image maps (OIMs) were acquired over an area of 1000 x 250 μm^2 using a step size of 0.25 μm.

2.3.3. Parent β Reconstruction Method

Here we give a brief outline of the method used to automatically reconstruct the parent β microtexture from the inherited α_s microtexture obtained by EBSD analysis. A more detailed description of the method will be given in a future publication. There are 4 steps:

1) Separation of the α_p and α_s microtextures.

First we separate the α_p and α_s phases so that the reconstruction will only be performed on the α_s phase. This is achieved by firstly, applying an average band contrast to the α_p grains and α_s variants, which results in good contrast between the predominantly light α_p grains and darker α_s variants. A user defined threshold separates the majority of α_s variants. In a second step, the majority of the remaining α_s variants are separated on account of their smaller size compared to the α_p grains. An optional final step enables the user to accept or reject grains in order to resolve any remaining discrepancies.

2) Reconstruction of the parent β grain structure.

A grain reconstruction procedure is used to determine the extent of each parent β grain. This procedure reconstructs each grain in turn by examining misorientations between neighbouring α_s pixels to see if they belong to either the same variant or different variants inherited from the same parent grain. Pixels are deemed to be from the same variant if the misorientation is less than a defined value (typically 3°). Pixels from different variants are deemed to be inherited from the same parent grain if both the angle and the axis of the misorientation are close to those of the 5 specific misorientations that occur between α_s variants inherited from the same parent grain[4].

3) Determination of β orientations from unique solutions.

For each α_s variant, we calculate all the misorientations along the boundary between it and neighbouring variants in the same parent grain. Each of these experimental misorientations will be close to 1 of 11 remarkable identities[2]. The closest remarkable identity is assigned to each misorientation and the most common remarkable identity for the variant in question is found. For 8 of the 11 remarkable identities, there is a unique rotation characterizing the parent β orientation. If the most common remarkable identity is one of these 8, then the β orientation is calculated for each pixel in the variant by the appropriate rotation. This step of the process successfully reconstructs β orientations in the majority of α_s variants.

4) Determination of β orientations from multiple solutions.

In the final step, β orientations are calculated in the variants for which the most common remarkable identity gave multiple solutions. The appropriate solution is selected by comparison with a nearby β orientation from the same parent grain that was calculated in step 3.

3. Results and Discussion

Optical micrographs from the PSC samples are shown in Fig. 2. The microstructures were bimodal, consisting of α_p grains in a continuous matrix of very fine transformed β. The volume fraction of α_p in the initial microstructure specimen was 28%, which is the expected volume fraction at 1010°C based on β approach curves previously determined for this billet. The temperatures recorded in the specimens after deformation due to deformation heating, were 1024°C and 1033°C for $\varepsilon_{vm} = 0.64$ and $\varepsilon_{vm} = 1.23$ respectively. The expected equilibrium volume fraction of α_p is 14% at 1024°C and 10% at 1033°C. However, in the deformed specimens, there was only a slight decrease in the volume fraction of α_p; 25% for $\varepsilon_{vm} = 0.64$, and 24% for $\varepsilon_{vm} = 1.23$. This indicates that the kinetics of the α→β phase change in this temperature range and for a strain rate of $2s^{-1}$ are such that only small changes in the volume fraction of α_p can occur during deformation.

3.1. Microstructural Evolution in the α_p Phase

In the as-received billet and the initial microstructure, there was a tendency for non equiaxed and contiguous α_p grains to be aligned along the billet axis (ND). For $\varepsilon_{vm} = 0.64$, the α_p grains were more equiaxed and less contiguous and for $\varepsilon_{vm} = 1.23$, there was a tendency for the α_p grains to be slightly pancaked along RD. These relatively modest changes in the α_p phase are shown in Fig. 3, which plots the ratios between the mean linear intercept grain sizes in the RD and ND directions for each specimen. The equivalent strain accommodated by the α_p phase was estimated using equation 1, where A_1 and A_2 are the RD/ND aspect ratios of the α_p grains in the initial and deformed microstructures, respectively.

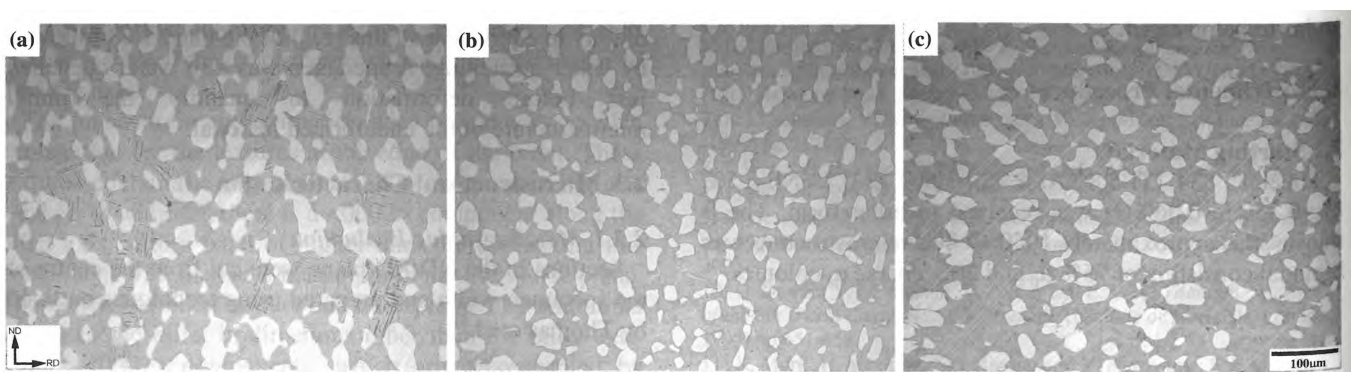

Figure 2. Optical microstructures of the PSC specimens: (a) initial microstructure, (b) $\varepsilon_{vm} = 0.64$, (c) $\varepsilon_{vm} = 1.23$.

$$\varepsilon_{vm\,\alpha_p} = \frac{\sqrt{3}}{2\sqrt{2}} \ln\left(\frac{A_2}{A_1}\right) \quad (1)$$

This approach showed that for the ε_{vm} = 1.23 specimen, the α_p phase undergoes an average strain of only 0.16. This behaviour is typical of titanium alloys deformed in the α+β phase field at temperatures at which β becomes the continuous phase, where the isolated α particles behave like hard inclusions in the soft β matrix [6].

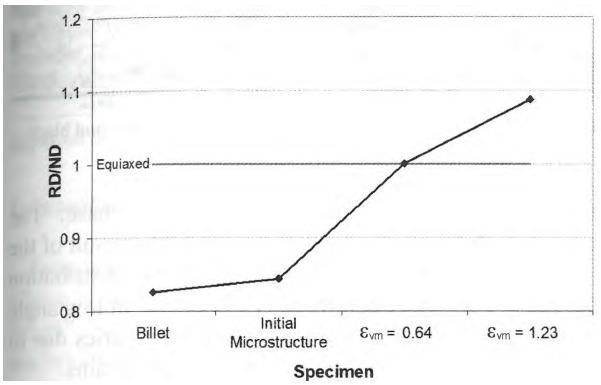

Figure 3. Ratio of α_p RD/ND mean linear intercept grain size for the as-received billet and the PSC specimens.

EBSD band contrast maps showing low and high angle grain boundaries in the α_p grains are shown in Fig. 4. In the initial microstructure (Fig. 4a), smaller α_p grains generally contained no substructure, while larger α_p grains were generally divided into subgrains separated by low angle grain boundaries. Both low and high angle boundaries were observed between contiguous α_p grains. Accumulated misorientations across the interior of the subgrains were low, which is indicative of a low dislocation density. In addition, the subgrain boundaries are clearly visible in the band contrast maps as sharp boundaries even for misorientations as low as 1°. These features suggest a well recovered microstructure.

In the ε_{vm} = 0.64 specimen (Fig. 4b), accumulated misorientations across the subgrains and grains were higher and there was an increase in substructure compared to the initial microstructure. Strain in the α_p phase was heterogeneous between α_p grains and within the grains themselves. Some grains showed only modest increases in accumulated misorientations and substructure, whereas in other grains it was much higher. Where the level of substructure was high, it often appeared to be composed of fine equiaxed cells approximately 2μm in diameter. Within the α_p grains, the substructure and accumulated misorientations were often concentrated within a smaller area of the grain. These areas were almost always at the edge of the grain and were often located around the boundary with a neighbouring grain. A small number of deformation twins were observed in α_p grains but the overall contribution of this mechanism to the strain in the α_p was very low.

The ε_{vm} = 1.23 specimen (Fig. 4c) showed a further increase in accumulated misorientations and substructure within the α_p grains. There was no significant increase in the level of deformation twinning. In some grains, where there was heavy localized deformation, recrystallized areas of fine equiaxed high angle grains (~2 μm in diameter) developed from the cell like substructure. The high misorientations between these grains suggest that they have dynamically recrystallized, perhaps by a form of continuous dynamic recrystallization[7]. However, the volume fraction of these recrystallized areas was low. The recrystallized areas were most common in small or thin α_p grains but were also observed at the edges of larger α_p grains and on boundaries between contiguous α_p grains.

3.2. Microstructural Evolution in the β Phase

EBSD maps for the reconstructed β phase, showing low and high angle grain boundaries are shown in Fig. 5. In the initial microstructure (Fig. 5a), the grain size is controlled by the pinning of the α_p phase. In common with the α_p grains, they therefore tend to be non equiaxed and aligned along the billet axis (ND). Several neighbouring grains frequently share similar orientations, with only low angle grain boundaries between them. Since the grains are newly formed during the heat treatment, they contain no substructure.

The deformed maps (Fig 5b and 5c) clearly show the large strains accommodated by the β phase during deformation. Large deformed β grains containing substructure can be seen to be pancaked along RD. Along the boundaries of the deformed grains are smaller more

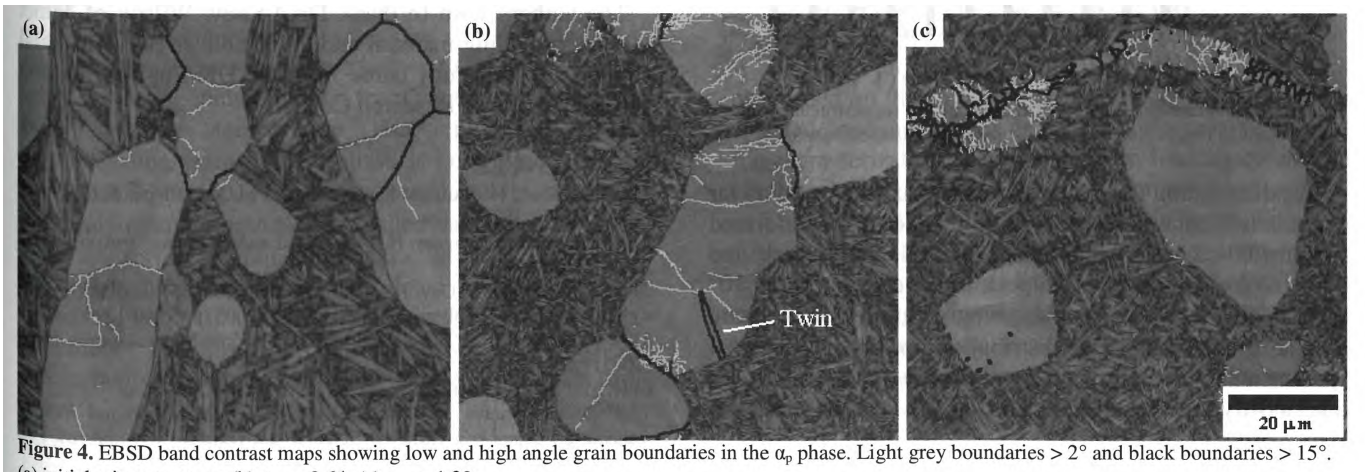

Figure 4. EBSD band contrast maps showing low and high angle grain boundaries in the α_p phase. Light grey boundaries > 2° and black boundaries > 15°. (a) initial microstructure, (b) ε_{vm} = 0.64, (c) ε_{vm} = 1.23.

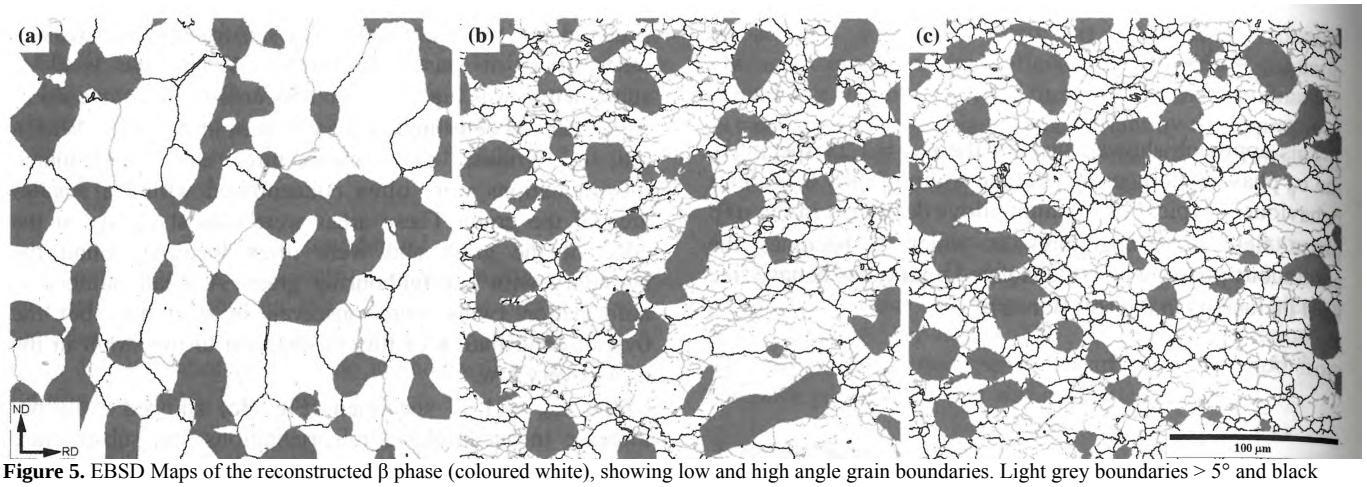

Figure 5. EBSD Maps of the reconstructed β phase (coloured white), showing low and high angle grain boundaries. Light grey boundaries > 5° and black boundaries > 15°. (a) initial microstructure, (b) $\varepsilon_{vm} = 0.64$, (c) $\varepsilon_{vm} = 1.23$.

equiaxed grains with mostly high angle grain boundaries. These microstructures resemble the necklace-like structure of a dynamically recrystallizing microstructure, where the new grains nucleate on the grain boundaries of the older deformed grains. It can be seen that the β phase recrystallizes quite heterogeneously, which is indicative of the inhomogeneous nature of the deformation in the β phase due to the accommodation strains imposed by the harder α_p grains. The recrystallized grains in the deformed specimens are approximately 10-20 µm in diameter. The percentage of the β phase that has recrystallized is approximately 20% in the $\varepsilon_{vm} = 0.64$ specimen, and approximately 45%; .in the $\varepsilon_{vm} = 1.23$ specimen.

Misorientation angle distributions in the reconstructed β phase were calculated from the EBSD maps (Fig. 6). Misorientations below 5° degrees were excluded from the distributions because it is difficult to differentiate between real misorientations and orientation noise at low angles.

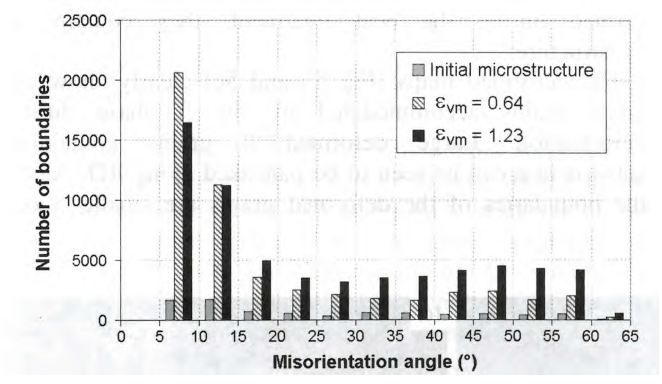

Figure 6. Misorientation angle distribution in the reconstructed β phase for the maps in Fig. 5. Note: no data is given for misorientations < 5°.

The distribution for the initial microstructure contains far fewer misorientations above 5° compared to the deformed specimens because the β grains are relatively large and contain no substructure. The peak in the distribution at 10° reflects the fact that neighbouring β grains often share similar orientations. The distribution for the $\varepsilon_{vm} = 0.64$ specimen shows the highest level of low angle boundaries due mostly to the substructure within the deformed β grains, which form the majority of the β phase. The increase in higher misorientations is mainly the result of the new dynamically recrystallized grains. In the distribution for the $\varepsilon_{vm} = 1.23$ specimen there is a decrease in low angle boundaries and an increase in high angle boundaries due to the increasing volume fraction of recrystallized grains.

4. Conclusions

For Timetal® 834 at a forging temperature of 1010°C, where the microstructure consists of α_p grains in a continuous β matrix, the overall strain accommodated by the α_p phase is low, with the majority of the strain accommodated by the softer β phase.

Deformation in the α_p phase is heterogeneous between grains and within the grains themselves. Deformation twinning was observed but does not contribute significantly to deformation. For practical purposes, the α_p phase remains unrecrystallized even at high strains. However in a few localized areas of heavy deformation a form of dynamic recrystallization was observed.

Deformation in the β phase is also heterogeneous due to the accommodation strains imposed by the α_p grains. The β phase dynamically recrystallizes but at the relatively high equivalent strains of 1.23 remained only partially recrystallized.

Acknowledgement

The authors wish to thank Dr. Andrew Wilson of Timet UK for providing material and invaluable advice. Financial support for this study came from the UK Engineering and Physical Sciences Research Council.

REFERENCES

1) M. Humbert, H. Mustafa, F. Wagner and M. J. Philippe: Scr. Met. **30** (1994) pp.377-382.
2) M. Humbert, F. Wagner, **H.** Moustahfid and C. Esling: J. Appl. Cryst. **28** (1995) pp.571-576.
3) M. Humbert and N. Gey: J. Appl. Cryst. **35** (2002) pp.401-405.
4) N. Gey and M. Humbert: J. Mater. Sci. **38** (2003) pp.1289-1294.
5) M. J. Thomas, **B.** P. Wynne and W. M. Rainforth: Mater. Charact. **55** (2005) pp. 388-394.
6) H. M. Flower: Mater. Sci. Tech. **6** (1990) pp.1082-1092.
7) F. J. Humphreys and M. Hatherly: *Recrystallization and Related Annealing Phenomena*, (Elsevier Science Ltd, Oxford, 1996) pp.167-171.